Neuron, Vol. 31, 247–260, August 2, 2001, Copyright ©2001 by Cell Press

The Expression of Vesicular Glutamate Transporters Defines Two Classes of Excitatory Synapse

Robert T. Fremeau, Jr.,[1] Matthew D. Troyer,[1] Ingrid Pahner,[2] Gro Owren Nygaard,[2] Cindy H. Tran,[1] Richard J. Reimer,[1] Elizabeth E. Bellocchio,[1] Doris Fortin,[1] Jon Storm-Mathisen,[2] and Robert H. Edwards[1,3]

[1] Departments of Neurology and Physiology
Graduate Programs in Neuroscience, Cell Biology, and Biomedical Sciences
513 Parnassus Avenue
UCSF School of Medicine
San Francisco, California 94143

[2] Department of Anatomy
IMBA
University of Oslo
Sognsvannsveien 9
P.O. Box 1105 Blindern
N-0317 Oslo
Norway

Summary

The quantal release of glutamate depends on its transport into synaptic vesicles. Recent work has shown that a protein previously implicated in the uptake of inorganic phosphate across the plasma membrane catalyzes glutamate uptake by synaptic vesicles. However, only a subset of glutamate neurons expresses this vesicular glutamate transporter (VGLUT1). We now report that excitatory neurons lacking VGLUT1 express a closely related protein that has also been implicated in phosphate transport. Like VGLUT1, this protein localizes to synaptic vesicles and functions as a vesicular glutamate transporter (VGLUT2). The complementary expression of VGLUT1 and 2 defines two distinct classes of excitatory synapse.

Introduction

Excitatory neurotransmission involves the exocytotic release of synaptic vesicles filled with glutamate. Glutamate is synthesized in the cytoplasm and undergoes transport into synaptic vesicles for quantal release. Like the uptake of other classical transmitters, vesicular glutamate transport depends on a proton electrochemical gradient ($\Delta\mu_{H+}$) generated by the vacuolar H^+-ATPase (Disbrow et al., 1982; Naito and Ueda, 1983). However, unlike the uptake of monoamines and acetylcholine (ACh), vesicular glutamate transport relies predominantly on the electrical component of this gradient ($\Delta\Psi$) rather than the chemical component (ΔpH) (Carlson et al., 1989a; Maycox et al., 1988). Consistent with this different mechanism, the two protein families responsible for vesicular uptake of monoamines, ACh and γ-aminobutyric acid (GABA) (Liu and Edwards, 1997a; Reimer et al., 1998; Schuldiner et al., 1995; Varoqui et al., 1994) have not been found to include a glutamate transporter.

Recent work has shown that a protein originally considered to perform an entirely different function in fact transports glutamate into synaptic vesicles (Otis, 2001). The brain-specific Na^+-dependent phosphate transporter (BNPI) was initially identified as a sequence upregulated in neurons by subtoxic concentrations of N-methyl-D-aspartate (Ni et al., 1994). Expressed in *Xenopus* oocytes, BNPI confers Na^+-dependent uptake of inorganic phosphate (Pi) and was suggested to have a role in the maintenance of energy stores (Glinn et al., 1997, 1998). However, the selective expression of BNPI by only glutamate neurons (Ni et al., 1995) raised the possibility of a more specific role in excitatory transmission. Genetic studies in *C. elegans* supported a role for the BNPI ortholog *eat-4* in glutamate release (Avery, 1993; Lee et al., 1999). The *eat-4* mutant has a specific defect in glutamatergic transmission (Raizen and Avery, 1994) but shows normal sensitivity to iontophoretically applied glutamate (Dent et al., 1997), further indicating a presynaptic defect. Consistent with a role in glutamate release, rat BNPI localizes to excitatory nerve terminals and specifically to synaptic vesicles (Bellocchio et al., 1998).

Although Pi uptake may have a specific role in glutamate production and release (Bellocchio et al., 1998), BNPI belongs to the type I class of Pi transporters that appear to have functions in addition to Pi transport. In particular, other type I Pi transporters recognize organic anions with higher affinity than Pi (Bröer et al., 1998; Busch et al., 1996; Mancini et al., 1989; Verheijen et al., 1999). These observations suggested that BNPI might also have a function distinct from Pi uptake. In recent work, we and others have found that BNPI transports glutamate into secretory vesicles with all of the properties previously demonstrated for glutamate uptake by native synaptic vesicles (Bellocchio et al., 2000; Takamori et al., 2000). In addition, heterologous expression of BNPI converts inhibitory GABAergic neurons to an excitatory phenotype (Takamori et al., 2000). We therefore renamed BNPI vesicular glutamate transporter 1 (VGLUT1). However, VGLUT1 is expressed by only a subset of glutamate neurons in the cortex, hippocampus, and cerebellum, raising questions about the mechanism by which excitatory neurons in the thalamus, brainstem, and elsewhere accumulate glutamate in synaptic vesicles.

We now show that a second protein recently identified as a novel type I Pi transporter also transports glutamate into synaptic vesicles. Induced during the differentiation of exocrine pancreas AR42J cells into neuroendocrine cells capable of insulin secretion, this differentiation-associated Na^+-dependent Pi transporter (DNPI) shows strong sequence similarity to VGLUT1 (Aihara et al., 2000). Like VGLUT1, its expression is restricted to the nervous system and it confers Na^+-dependent Pi uptake when expressed in *Xenopus* oocytes (Aihara et al., 2000). We now demonstrate by in situ hybridization that DNPI is expressed by essentially all glutamate neurons not

[3] Correspondence: edwards@itsa.ucsf.edu

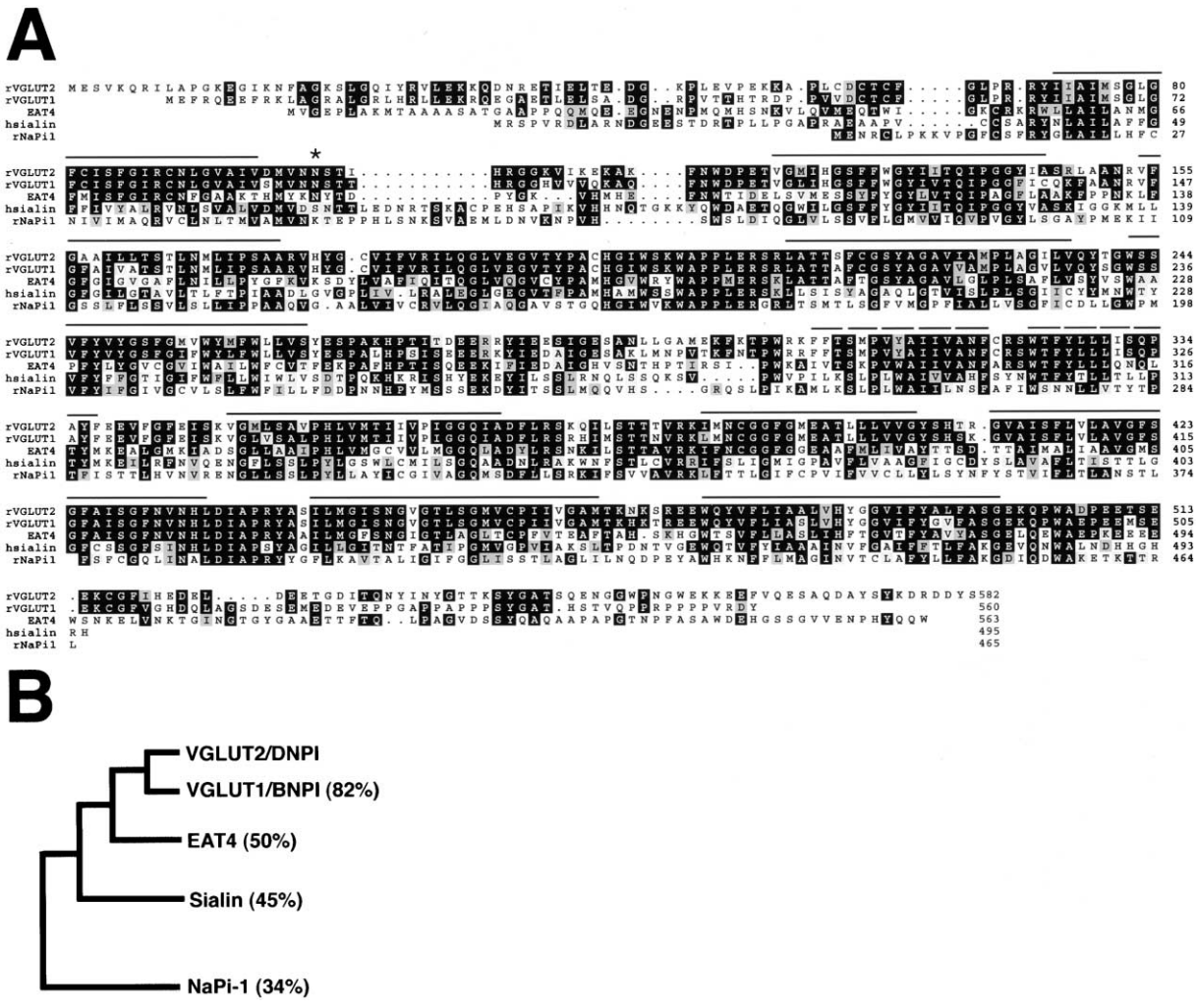

Figure 1. DNPI Belongs to a Subfamily of Type I Phosphate Transporters

(A) The predicted amino acid sequence of rat DNPI/VGLUT2 shows more similarity to rat VGLUT1 and *C. elegans* EAT-4 than to other type I phosphate transporters including human sialin and rat NaPi-1. The sequences were aligned using PILEUP (GCG). Black boxes indicate identical residues, and gray boxes indicate conservative substitutions. The solid lines above rat DNPI/VGLUT2 reflect the location of putative transmembrane domains (predicted by Kyte-Doolittle analysis of hydropathy). The dashed lines indicate hydrophobic segments too short to span the membrane that might form reentrant loops. The asterisk indicates a putative glycosylation site.

(B) Dendrogram showing the amino acid sequence relationship between rat VGLUT2 and rat VGLUT1, *C. elegans* EAT4, human sialin, and rabbit NaPi-1. The percentage shown in parentheses indicates the percent identity to rat VGLUT2.

expressing VGLUT1, and in particular by neurons in the thalamus, hypothalamus, and brainstem. Using an antibody that we raised to the protein, immunocytochemistry supports the localization of DNPI to synapses that appear largely distinct from those labeled for VGLUT1. In addition, we establish the localization of DNPI to synaptic vesicles by differential centrifugation, velocity gradient fractionation, and immunoelectron microscopy. Further, heterologous expression of DNPI in PC12 cells confers vesicular glutamate transport with properties very similar to native synaptic vesicles and VGLUT1. We have thus renamed DNPI vesicular glutamate transporter 2 (VGLUT2). The expression of distinct VGLUT isoforms by complementary populations of excitatory neurons suggests that they define distinct modes of glutamate release.

Results

DNPI more closely resembles VGLUT1 than other type I phosphate transporters such as NaPi-1 and sialin (Figure 1), suggesting that it may also transport glutamate into synaptic vesicles. In addition, DNPI is expressed selectively in the nervous system (Aihara et al., 2000) where it appears to have a distribution different from VGLUT1 (Hisano et al., 2000).

Complementary Expression by Excitatory Neurons

To determine whether DNPI is expressed by excitatory neurons that do not express VGLUT1, we examined the distribution of the two transcripts in adjacent brain sections by in situ hybridization. The closely related sequences were distinguished using probes from the 3′

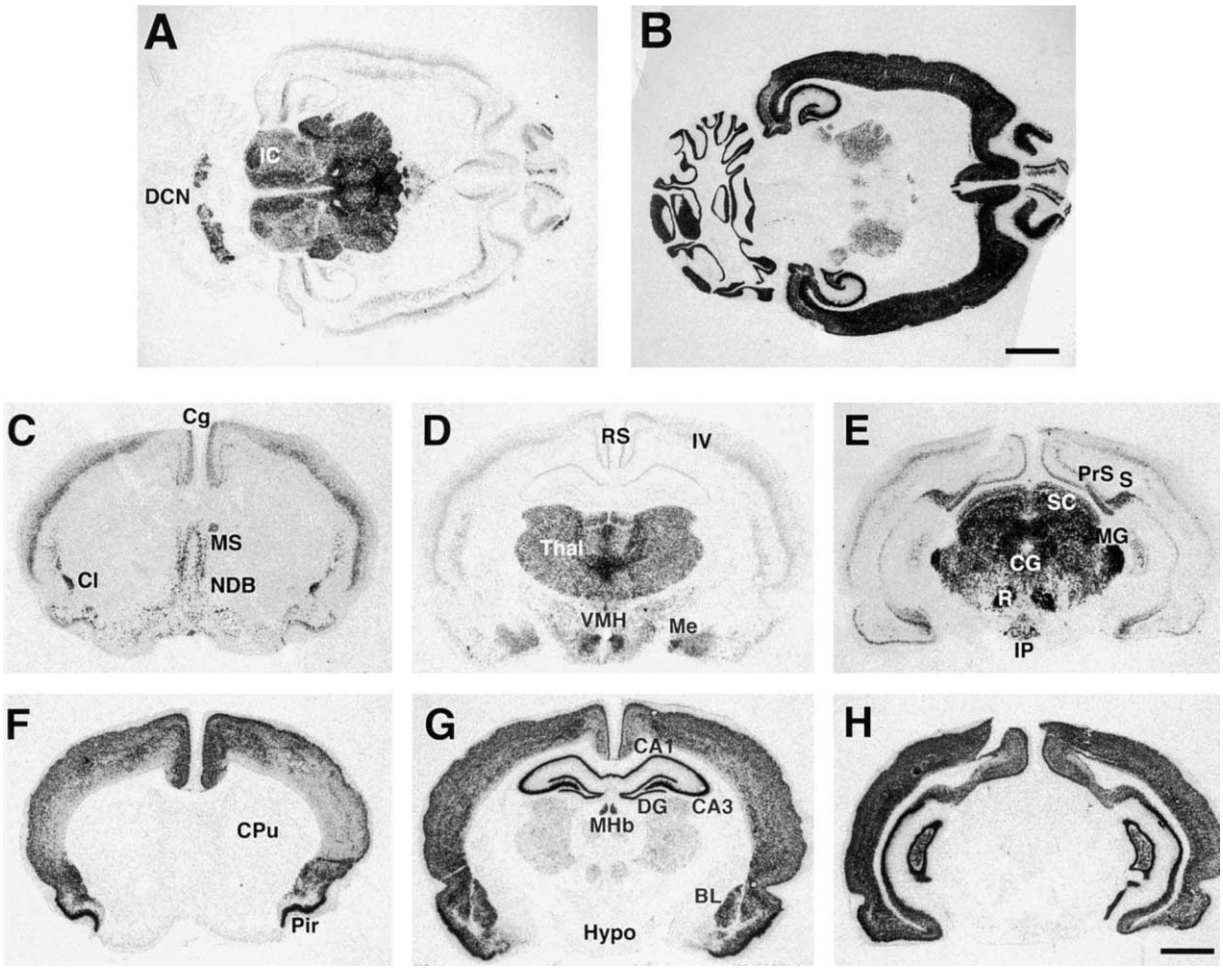

Figure 2. Differential Expression of DNPI and VGLUT1 by In Situ Hybridization

Horizontal (A and B) and coronal (C–H) brain sections from 3-week-old rats were hybridized with ^{35}S-labeled antisense RNA probes derived from unique carboxy-terminal and 3′ untranslated regions of rat DNPI/VGLUT2 (A and C–E) or VGLUT1 (B and F–H) cDNAs and exposed to film for 3 days. The cortex, hippocampus, and cerebellar cortex express predominantly VGLUT1, whereas the thalamus, brainstem, and deep cerebellar nuclei (DCN) express predominantly DNPI. Within the cortex, DNPI is expressed predominantly by neurons in layer IV, whereas VGLUT1 is expressed by layers II–VI. The caudate-putamen (CPu), containing largely inhibitory neurons, expresses neither sequence (C and F). In addition, the medial septum (MS), nuclei of the diagonal band (NDB), and hypothalamus (Hypo) express only DNPI (C). Within the hippocampus, DNPI occurs at low levels in the pyramidal cell layer relative to VGLUT1, but is slightly higher in CA1 and 2 than in other fields and is undetectable in the dentate gyrus (DG). In contrast, VGLUT1 shows robust expression by pyramidal neurons and granule cells in all areas (G). Numerous thalamic (Thal) and hypothalamic nuclei (such as the ventromedial nucleus, VMH) express DNPI but very little VGLUT1 (D and G). In the amygdala, the medial nucleus (Me) hybridizes exclusively for DNPI, whereas the lateral and basolateral (BL) nuclei hybridize more strongly for VGLUT1. Abbreviations not defined above: Cg, anterior cingulate cortex; Cl, claustrum; RS, retrospenial cortex; PrS, presubiculum; S, subiculum; SC, superior colliculus; MG, medial geniculate; CG, central gray; R, red nucleus; IP, interpeduncular nucleus; Pir, piriform cortex; MHb, medial habenula. Scale bars: 2 mm (A and B), 1.25 mm (C–H).

end of the protein-coding regions (and part of the 3′ untranslated regions), where the cDNAs are divergent. Further, longer probes containing more of the shared protein-coding sequence hybridized in a distribution identical to the shorter probes. The discrete patterns of hybridization observed also indicate essentially no cross-reactivity between the two sequences. On horizontal sections, the brainstem labels strongly for DNPI and very little if at all for VGLUT1 (Figures 2A and 2B). In the cerebellum, the cortex hybridizes to VGLUT1 but not to DNPI, whereas the deep nuclei hybridize selectively to DNPI. Thus, the pattern of expression appears largely complementary. The analysis of coronal sections further shows that the septal nuclei, nuclei of the diagonal band, hypothalamus, and the midbrain express DNPI but not VGLUT1 (Figures 2C–2H).

Several brain regions express both DNPI and VGLUT1, but in most of these, one transcript predominates and the patterns of expression remain distinct. All cortical layers label strongly for VGLUT1, whereas only layer IV of frontal and parietal cortex and layers IV and VI of temporal cortex label for DNPI (Figure 2). In the hippocampus, dentate gyrus granule cells contain only VGLUT1 mRNA (Figure 2G). Pyramidal neurons from CA1 through CA3 also express abundant VGLUT1, but lower levels of DNPI occur as well (Figures 2D). CA1 in particular labels for DNPI more strongly than other hippocampal fields, but the subiculum and presubiculum contain

abundant DNPI mRNA (Figure 2E). The thalamus expresses much more DNPI than VGLUT1 (Figure 2D), but certain thalamic nuclei such as the medial habenula hybridize to VGLUT1 (Figure 2G). In the amygdala, the medial and central nuclei contain abundant mRNA for DNPI, and the lateral and basolateral nuclei for VGLUT1 (Figures 2D and 2G). Expression of the two transcripts thus appears largely segregated to distinct neuronal populations.

We have not detected any discrete population of excitatory neurons that does not express either VGLUT1 or DNPI. We have also not detected any expression of DNPI or VGLUT1 by nonglutamatergic neurons. The caudate-putamen, which contains largely inhibitory projection neurons and cholinergic interneurons, lacks hybridization signal for either sequence (Figures 2C and 2F). Similarly, Purkinje cells in the cerebellum and other inhibitory neurons in the cerebellar cortex and hippocampus do not express detectable levels of either transcript (data not shown). Further, monoamine cell groups in the substantia nigra, locus coeruleus and raphe nuclei, and motor nuclei in the brainstem do not express detectable DNPI or VGLUT1 transcripts.

Localization to Excitatory Synapses

To determine whether DNPI localizes to excitatory synapses like VGLUT1 (Bellocchio et al., 1998), we raised an antibody to a bacterial fusion protein containing the cytoplasmic C terminus of the rat protein. The domain used to produce the antisera shows very little similarity to the corresponding carboxy-terminal domain from VGLUT1, sialin, or NaPi-1 (Figure 1). By Western analysis, the antibody recognizes DNPI but not VGLUT1 stably expressed in PC12 cells (Figure 7A). Nonetheless, to ensure specificity, we adsorbed both the DNPI antibody with the VGLUT1 fusion protein (Bellocchio et al., 1998) and the VGLUT1 antibody with the DNPI fusion protein. The distinct patterns of immunostaining observed for each antibody indeed confirm the lack of cross-reactivity. In contrast to the detection of VGLUT mRNA in cell bodies, the VGLUT proteins localize to processes.

Although brain regions such as the caudate-putamen label with both antibodies, presumably due to the expression of DNPI and VGLUT1 by distinct afferents, the immunoreactivity in many other areas appears segregated (Figure 3). The neocortex stains more strongly overall for VGLUT1 than DNPI, but layers IV and VI stain for DNPI and the VGLUT1 immunoreactivity appears less intense in these layers (Figures 3A and 3B). In addition, the piriform cortex stains more strongly for VGLUT1 than DNPI. The septal region also shows opposing gradients of labeling, with more VGLUT1 laterally and DNPI alone in the medial septum and nuclei of the diagonal band. At the level of the diencephalon, particular thalamic nuclei exhibit strong labeling for DNPI. Figure 3C shows that the midline, intralaminar and, to a lesser extent, lateral geniculate, ventroposterior medial, and lateral nuclei stain more strongly for DNPI than the posterior nucleus. Conversely, the lateral nuclei stain more strongly for VGLUT1 than medial nuclei (Figure 3D). The hypothalamus also shows more immunoreactivity for DNPI than VGLUT1, but with discrete areas of increased VGLUT1 labeling such as the ventromedial (Figure 3D) and mammillary nuclei (Figure 3F). The amygdala stains almost equally with the two antibodies, with slight differences in pattern. At the level of the midbrain, the DNPI antibody produces widespread labeling, with VGLUT1 detectable only in the medial geniculate nucleus of the thalamus (Figures 3E and 3F). Layers I and III of the presubiculum stain strongly and selectively for DNPI, likely reflecting commissural afferents from neurons in the contralateral presubiculum (van Groen and Wyss, 1990) that express DNPI mRNA (Figure 2E). In contrast, layer II and the subiculum stain preferentially for VGLUT1. DNPI and VGLUT1 thus exhibit complementary patterns of protein as well as mRNA expression.

Consistent with expression at synapses, DNPI localizes to punctate structures in the neuropil (Figure 4). In the hippocampus, the pyramidal cell layer of CA2 shows puncta immunoreactive for DNPI, whereas VGLUT1-positive puncta are distributed uniformly in stratum oriens and radiatum throughout CA1–3 (Figures 4A and 4B). Although CA1 and 3 do not generally contain DNPI immunoreactivity, stratum lacunosum-moleculare immunostains strongly for DNPI in the temporal fields of CA1 (Figure 3E), suggesting expression by afferents from the midline reuniens nucleus of the thalamus as well as the entorhinal cortex (Wouterlood et al., 1990), both of which express DNPI mRNA (Figure 2). In the dentate gyrus, DNPI again localizes specifically to nerve terminals in the granule cell layer with VGLUT1 in other layers (Figures 4C and 4E). Since the granule cell layer of the dentate gyrus shows no signal for DNPI by in situ hybridization (Figure 2D), this distribution suggests a presynaptic location. Supporting this possibility, cells in the hypothalamus that project to this layer (Amaral and Witter, 1995; Wyss et al., 1979) strongly express DNPI mRNA. Further, immunoperoxidase staining shows DNPI expression in nerve terminals by electron microscopy (Figure 4C).

The molecular layer of the cerebellum contains immunoreactivity for DNPI as well as VGLUT1 (Figures 4F–4H). Dendrites in this layer derive predominantly from inhibitory Purkinje cells or interneurons, which do not express either DNPI or VGLUT1 mRNA. DNPI-immunoreactive puncta in the molecular layer thus most likely represent expression at nerve terminals. In particular, the DNPI antibody labels climbing fibers (Figure 4F) derived from inferior olivary neurons that express DNPI transcripts. In contrast, the VGLUT1 antibody stains parallel fibers (Figure 4H) originating from granule cells that express VGLUT1 mRNA. Thus, the two major classes of excitatory synaptic input onto Purkinje cells show complementary expression of DNPI and VGLUT1. Both DNPI and VGLUT1 also localize to mossy fiber terminals in the granular layer of the cerebellum (Figures 4F and 4H), consistent with the origin of mossy fibers from many different CNS regions.

Localization to Synaptic Vesicles

The expression of DNPI at synapses and in particular on nerve terminals suggests that it may localize to synaptic vesicles, similar to VGLUT1 (Bellocchio et al., 1998). We have therefore used biochemical fractionation of brain extracts to determine the subcellular location of DNPI. Figure 5A shows progressive enrichment of the synaptic

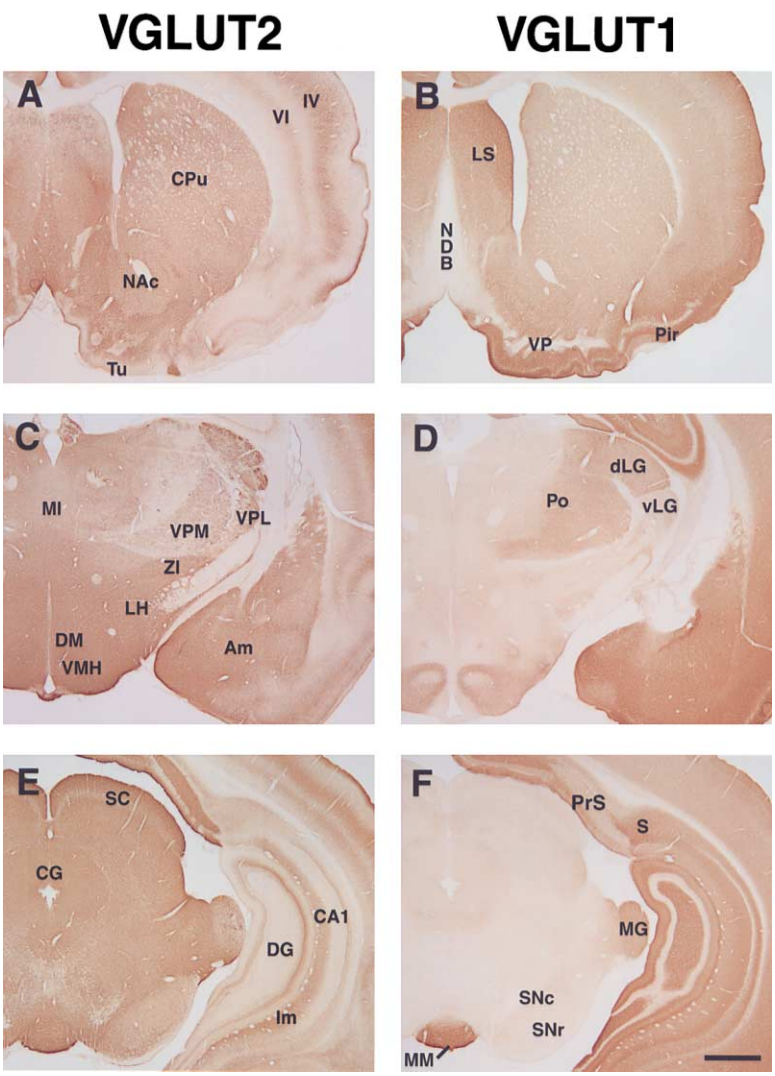

Figure 3. Complementary Expression of VGLUT Proteins in Synaptic Layers

Adjacent rat brain sections were immunostained using the peroxidase method for DNPI/VGLUT2 (A, C, and E) and VGLUT1 (B, D, and F). In all regions, the immunoreactivity for both proteins appears punctate and restricted to gray matter, suggesting expression at synapses. At the level of the caudate-putamen (CPu) and nucleus accumbens (NAc) (A and B), the striatum labels for both proteins, but DNPI clearly predominates in the ventral pallidum and nucleus of the diagonal band (NDB). In the cortex, DNPI localizes to layers IV and VI, and VGLUT1 to all layers. (Tu = olfactory tubercle, Pir = piriform cortex). At the level of the caudal diencephalon (C and D), DNPI immunoreactivity is much more prominent than VGLUT1 in thalamic nuclei, particularly medial and intralaminar nuclei (MI), and in hypothalamic nuclei, especially the dorsomedial (DM) and lateral nuclei (LH). Sensory relay nuclei of the thalamus, including the ventroposteromedial nucleus (VPM), ventroposterolateral nucleus (VPL), and the lateral geniculate (LG) nucleus label for both proteins. However, these nuclei vary in the extent of labeling, with VPM and VPL nuclei more strongly immunoreactive for DNPI than the posterior (Po) nucleus and the dorsal lateral geniculate (dLG) more reactive for VGLUT1 than the ventral lateral geniculate (vLG) and zona incerta (ZI). Both DNPI and VGLUT1 are found throughout the amygdaloid complex (Am). At the level of the midbrain (E and F), most brainstem structures lack VGLUT1 immunoreactivity, whereas the midbrain shows widespread staining for DNPI in the superior colliculus (SC), central gray (CG), substantia nigra pars compacta (SNc), and substantia nigra pars reticulata (SNr). The mammillary nucleus (MM) and medial geniculate body (MG) contain both proteins. The presubiculum (PrS, notably layer III), but not the subiculum (S), strongly labels for DNPI, whereas VGLUT1 shows the opposite pattern of immunoreactivity. Distinct, complementary patterns of immunostaining are present in the hippocampus (see also Figure 4). Although VGLUT1 immunoreactivity predominates, stratum lacunosum-moleculare (lm) also contains DNPI. Preadsorption with the VGLUT2-GST fusion protein eliminated the immunoreactivity observed with DNPI antibody (see Figure 4). Scale bar: 1 mm (all panels).

vesicle protein synaptophysin in the light membranes (fraction LP2) derived from hypotonic lysis of synaptosomes (Huttner et al., 1983). Both DNPI and VGLUT1 show a similar enrichment in this fraction. In contrast, the plasma membrane protein syntaxin and a subunit of the NMDA receptor (NR1) sediment with heavy membranes released by synaptosome rupture (LP1). The localization of DNPI to LP2 thus supports specific expression on synaptic vesicles. However, relative to synaptophysin, DNPI and VGLUT1 were also detected in substantial amounts in LP1, consistent with expression on heavy membranes such as the plasma membrane in addition to synaptic vesicles (Figure 5A). Further, DNPI shows greater localization than VGLUT1 to a population of crude membranes lighter than synaptosomes (S2).

To confirm the expression of DNPI on synaptic vesicles, we have used velocity sedimentation through a glycerol gradient. This fractionation procedure separates synaptic vesicles from essentially all other membranes present in lysed synaptosomes (Clift-O'Grady et al., 1990), and we find the anticipated peak of synaptophysin near the top of this gradient (Figure 5B). Smaller amounts of synaptophysin reside in the pellet. Similarly, DNPI and VGLUT1 comigrate with synaptophysin at the top of this gradient, indicating expression on synaptic vesicles. In contrast, syntaxin appears at very low levels in these fractions relative to the bottom of the gradient, supporting expression at the plasma membrane. Although DNPI and VGLUT1 are clearly enriched in synaptic vesicles relative to syntaxin, the two related proteins also reside at higher levels on the bottom of the gradient than synaptophysin. Velocity sedimentation thus supports the results of differential centrifugation indicating expression of DNPI predominantly on synaptic vesicles, with lesser amounts on other membranes such as the plasma membrane.

Immunoelectron microscopy confirms the biochemical analysis of DNPI localization. Labeling with gold par-

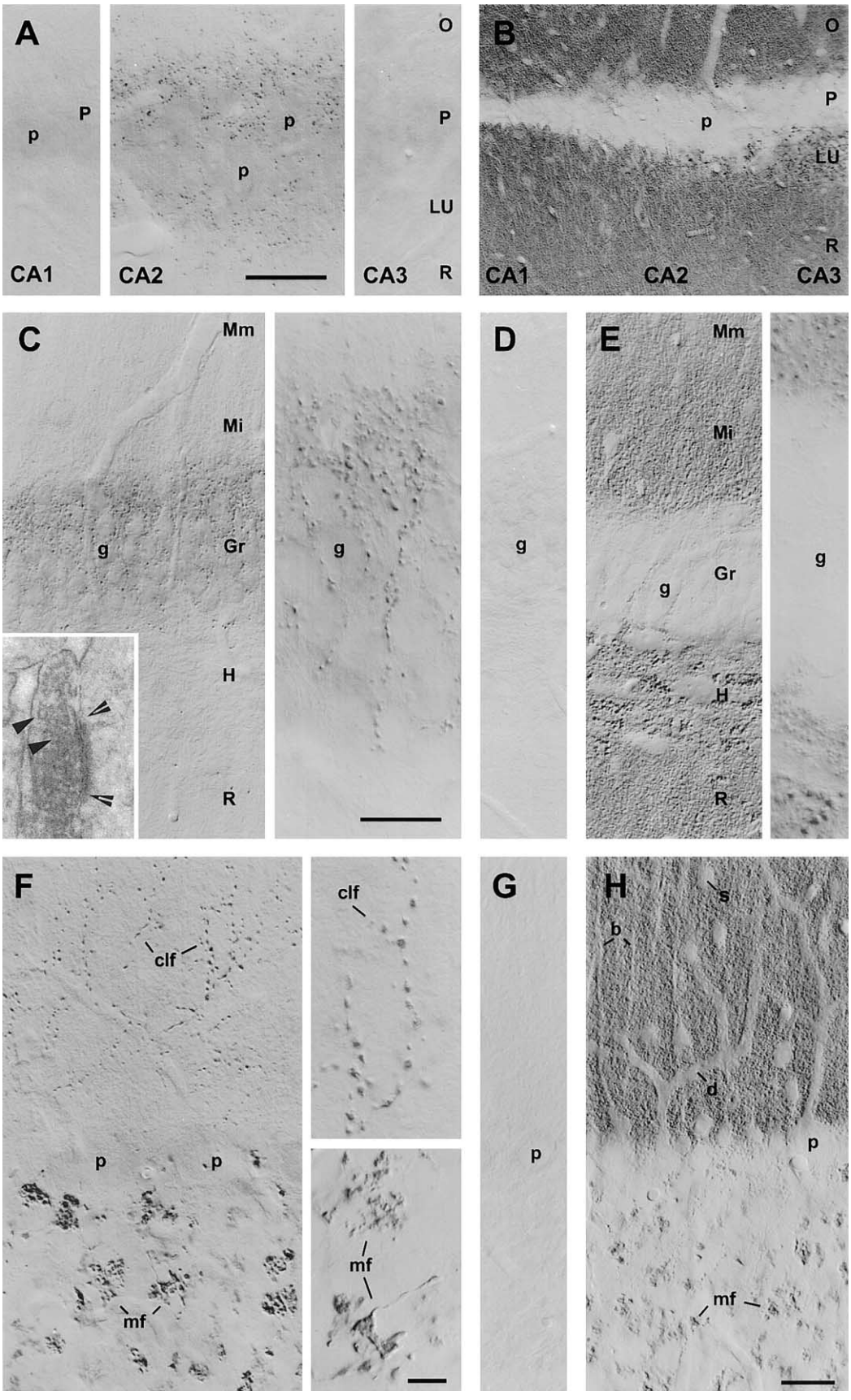
A
P
p
CA1
p
p
CA2
O
P
LU
R
CA3
B
O
P
p
LU
R
CA1
CA2
CA3
C
Mm
Mi
g
Gr
H
R
g
D
g
E
Mm
Mi
g
Gr
H
R
g
F
clf
p
p
mf
clf
mf
G
p
H
s
b
d
p
mf

ticles in the molecular layer of the cerebellar cortex shows DNPI on the synaptic vesicles of climbing fiber boutons, with no labeling of parallel fibers (Figure 6A). In contrast, VGLUT1 labels selectively the synaptic vesicles in parallel fibers but not those in climbing fibers (Figure 6B). The localization of DNPI to synaptic vesicles in specific excitatory nerve terminals suggested that DNPI might transport glutamate into synaptic vesicles, similar to VGLUT1 (Bellocchio et al., 2000; Takamori et al., 2000).

DNPI Transports Glutamate

To determine whether DNPI transports glutamate into secretory vesicles, we used heterologous expression in rat pheochromocytoma PC12 cells, which exhibit no endogenous DNPI mRNA or immunoreactivity (Figures 7A and 7B). We derived a series of transfected clones stably expressing DNPI, prepared a population of light membranes including synaptic-like microvesicles, and assayed their ability to accumulate [^{3}H]L-glutamate. Figure 8A shows that membranes prepared from cell clones 30 and 61 accumulate substantially more [^{3}H]L-glutamate than untransfected cells. As anticipated, this activity does not require Na^+, distinguishing DNPI from plasma membrane glutamate transporters. Figure 8B shows that the initial rate of glutamate uptake follows Michaelis-Menten kinetics and saturates with a Km 4.7 $\pm$ 0.7 mM ($n = 3$), slightly higher than that observed using native synaptic vesicles from the brain or VGLUT1 (Bellocchio et al., 2000; Naito and Ueda, 1983).

We also examined the substrate specificity and chloride dependence of glutamate uptake mediated by DNPI. Figure 8C shows that L-glutamate, but not L- or D-aspartate, glycine, or GABA (all 10 mM), markedly inhibits [^{3}H]L-glutamate uptake by DNPI (Figure 8C). D-glutamate and Evans Blue (4.5 μM) also inhibit uptake, as expected for a vesicular glutamate transporter (Figure 8C), but Pi does not (data not shown). Like native synaptic vesicles and VGLUT1 (Bellocchio et al., 2000), DNPI exhibits a biphasic dependence on chloride with an optimum concentration in the same range, 2–10 mM (Figure 8D) (Wolosker et al., 1996). In addition, dissipation of the electrical potential $\Delta\Psi$ across the vesicle membrane with the K^+ ionophore valinomycin inhibits [^{3}H]L-glutamate uptake more than dissipation of the pH gradient with nigericin (Figure 8E). DNPI thus also appears to depend on $\Delta\Psi$ to a greater extent than ΔpH. However, it is clear that DNPI, like VGLUT1, depends on ΔpH. Nigericin alone did not significantly reduce transport, but its addition to valinomycin essentially abolishes uptake. DNPI thus resembles VGLUT1 in transport activity.

In PC12 cells, the immunoreactivity for both DNPI and VGLUT1 is intracellular and colocalizes with synaptophysin in processes (Figures 7C–7H). However, we also observed a difference in the subcellular location of DNPI and VGLUT1. Within cell bodies, DNPI localizes diffusely throughout the cytoplasm (Figure 7C). In contrast, VGLUT1 has a more peripheral distribution, just beneath the plasma membrane (Figure 7F). We have observed this difference in multiple cell clones. Expressed in the same cells, DNPI and VGLUT1 thus appear to differ in trafficking, which may contribute to the differences in distribution observed by differential centrifugation.

Discussion

Although VGLUT1 catalyzes vesicular glutamate transport and is expressed by many excitatory neurons, many others do not express VGLUT1 (Bellocchio et al., 1998; Ni et al., 1995). We now show that the closely related DNPI is expressed by excitatory neurons negative for VGLUT1. In addition, DNPI cofractionates by differential centrifugation with synaptic vesicle proteins synaptophysin and VGLUT1, cofractionates by velocity sedimentation through glycerol with synaptic vesicles, and localizes to synaptic vesicles by immunoelectron microscopy. Further, heterologous expression of DNPI confers Na^+-independent glutamate uptake with a Km

Figure 4. Complementary Expression of VGLUT Proteins in the Hippocampus and Cerebellar Cortex

(A) In the hippocampus, DNPI/VGLUT2-immunoreactivity localizes selectively to nerve endings in the pyramidal layer (P) of CA2 (and immediately adjacent CA3), but not CA1 or CA3. Pyramidal cell bodies (p) are not immunoreactive.

(B) VGLUT1, in contrast, localizes throughout CA1–3 in small puncta distributed uniformly in strata oriens (O) and radiatum (R) (representing the terminals of the Schaffer collateral system from CA3 pyramidal cells), and in large, mossy fiber boutons in stratum lucidum (LU), representing the terminals of the axons from dentate granule cells (Storm-Mathisen et al., 1983).

(C) In the dentate gyrus, DNPI localizes selectively to nerve endings in the granular layer (Gr), particularly in its superficial parts. Granule cell bodies (g) are unstained. Right panel: high-magnification view of a different section under oil immersion. Inset: electron micrograph showing the synapse of an immunoreactive nerve terminal onto a dendrite in the granule cell layer; arrowheads indicate synaptic vesicles, open arrowheads point to synaptic site (Stanfield and Cowan, 1984).

(D and G) Preadsorption of DNPI serum with DNPI-GST fusion protein (20 μg/ml) abolishes the staining of nerve terminals.

(E) VGLUT1 localizes to small puncta in all the other layers of the dentate gyrus, including puncta in the molecular layer (with the middle zone [Mm] containing terminals of the medial perforant path, and the inner zone [Mi] terminals of mossy cells in the hilus [H]), and large, mossy fiber boutons. (Stratum radiatum [R] of CA3 appears near the bottom of the main panel.) Right panel: high-magnification view under oil immersion shows immunoreactive nerve endings in layers Mi and H. The distribution of DNPI/VGLUT2-immunoreactive boutons (A and C) conforms to the distribution of afferents from the supramammillary nucleus (Amaral and Witter, 1995), whereas the distribution of VGLUT1-immunoreactive boutons (B and E) conforms to that of the main glutamate immunoreactive systems (Storm-Mathisen et al., 1983).

(F) In the cerebellum, DNPI/VGLUT2 localizes to climbing fiber boutons (clf) in the molecular layer, and to mossy fiber boutons (mf) in the granule cell layer. Insets: high-magnification view under oil immersion showing clf, and two different shapes of mf.

(H) Dense VGLUT1-immunoreactive puncta representing parallel fiber boutons fill the molecular layer and show unstained structures in silhouette: Bergmann astroglia (b), Purkinje cell dendrites (d), and cell bodies (p), stellate interneurons (s), and blood vessels (not indicated). In addition, VGLUT1 is expressed in mossy fiber boutons (mf).

Sections were viewed by differential interference contrast (DIC) optics. Scale bar shown in (A): (A), all panels, (C–E), main panels, 50 μm; (B), 100 μm; (C and E), right panels, 20 μm; (C), inset, 0.3 μm. Scale bar in (F–H), 30 μm; (F), insets, 10 μm.

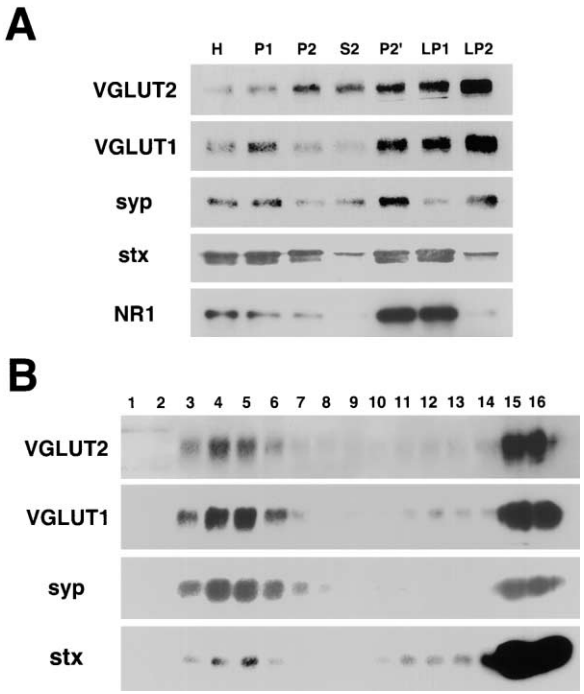

Figure 5. DNPI Localizes to Synaptic Vesicles

(A) After differential centrifugation of rat brain extracts prepared by the hypotonic lysis of synaptosomes (Huttner et al., 1983), equal amounts of protein from each fraction were analyzed by Western blotting. Like VGLUT1, DNPI/VGLUT2 cosediments with the synaptic vesicle protein synaptophysin (syp), the plasma membrane t-SNARE syntaxin (stx), and the NMDA receptor subunit NR1 in the washed synaptosome fraction P2′. After hypotonic lysis, both DNPI and VGLUT1 appear enriched in a population of light membranes (LP2) along with synaptophysin, whereas syntaxin and NR1 fractionate with heavier membranes (including the plasma membrane) in LP1. However, DNPI and VGLUT1 also appear at higher levels in LP1 than synaptophysin, suggesting localization on the plasma membrane as well as synaptic vesicles. In addition, DNPI appears at higher levels than VGLUT1 on a population of crude membranes lighter than synaptosomes (S2).

(B) Fractions 1–16 were collected from the top of a 5%–25% glycerol velocity gradient used to fractionate P2′ (Clift-O'Grady et al., 1990). Western analysis of equal volumes from each fraction shows that DNPI cofractionates with VGLUT1 and synaptophysin in fractions 3–7. In contrast, the plasma membrane protein syntaxin occurs predominantly at the bottom of the gradient. However, DNPI and VGLUT1 show proportionately more immunoreactivity at the bottom of the gradient than synaptophysin, suggesting expression on membranes in addition to synaptic vesicles.

$\sim$5 mM and a biphasic dependence on chloride. Glutamate transport by DNPI also depends on $\Delta\Psi$ to a greater extent than ΔpH. These properties resemble those previously observed for glutamate uptake by native synaptic vesicles from brain (Carlson et al., 1989a; Maycox et al., 1988). Since DNPI resides on synaptic vesicles and catalyzes vesicular glutamate transport, we propose the alternative name VGLUT2.

The expression of VGLUT1 and 2 mRNA transcripts appears complementary. Unlike the isoforms of many other synaptic vesicle proteins, which overlap extensively in distribution (Bajjalieh et al., 1993; Fykse et al., 1993), the VGLUTs exhibit distinct, generally nonoverlapping patterns of expression. Many neurons in the cortex express only VGLUT1, whereas most cells in the brainstem express only VGLUT2. In the cerebellum, the cortex expresses VGLUT1 and the deep nuclei VGLUT2. In other regions expressing both isoforms, one clearly predominates. Although most cortical layers express VGLUT1, neurons in layers IV and VI express VGLUT2. In addition, the thalamus expresses predominantly VGLUT2, but selected nuclei express low levels of VGLUT1. The complementary pattern of VGLUT1 and 2 expression appears to reflect segregated expression at the level of individual neurons. It remains to be determined whether there may also be cells that express both transcripts.

The expression of VGLUT1 and 2 accounts for the exocytotic release of glutamate by essentially all excitatory neurons. We have not observed any known population of excitatory neurons that does not express either isoform. In addition, nonglutamatergic cells do not express either VGLUT1 or 2. However, monoamine neurons have been reported to form glutamatergic autapses in culture, suggesting the expression of a vesicular glutamate transporter (Sulzer et al., 1998). Monoamine neurons may thus express a VGLUT isoform either transiently during development or after growth in vitro. Motor neurons have also been shown to exhibit quantal glutamate release after cytoplasmic loading with high concentrations of glutamate (Dan et al., 1994), but we have failed to detect either isoform in cranial motor nuclei. Further, we have not detected expression of VGLUT1 or 2 mRNA or protein by astrocytes, and considerable work has implicated glial cells in the exocytotic release of glutamate (Araque et al., 2000; Bezzi et al., 1998; Newman and Zahs, 1998). Glial cells may express VGLUT1 or VGLUT2, but at considerably lower levels that have eluded detection. Alternatively, cells not traditionally considered glutamatergic may express another, unidentified glutamate transporter.

The VGLUT proteins also appear segregated to distinct excitatory synapses. Layer IV of the cortex stains strongly for VGLUT2, consistent with the presence of afferents from thalamic nuclei expressing VGLUT2 mRNA. Layer VI also labels for VGLUT2, whereas other cortical layers stain more strongly for VGLUT1. In the thalamus, medial and intralaminar nuclei stain more heavily for VGLUT2, likely reflecting input from brainstem, hypothalamus, and deep cerebellar nuclei (Cornwall and Phillipson, 1988a, 1988b), which express VGLUT2 mRNA. Lateral nuclei label more strongly for VGLUT1, presumably derived from cortical afferents. Strikingly complementary synaptic staining also occurs in the presubiculum, subiculum, hippocampus, and cingulate cortex. Further, in the cerebellum, climbing fibers derived from the VGLUT2-positive inferior olive form synapses onto the same population of Purkinje cells contacted by parallel fibers derived from the VGLUT1-positive granule cells. Expression of the VGLUTs thus defines two populations of excitatory synapses.

Why do certain excitatory neurons express VGLUT1 and others VGLUT2? One possibility is that their distribution may simply reflect developmental history. In general, VGLUT1 appears expressed by structures derived from the telencephalon such as the cortex and hippocampus, and VGLUT2 by structures derived from the diencephalon and rhombencephalon. However, VGLUT1

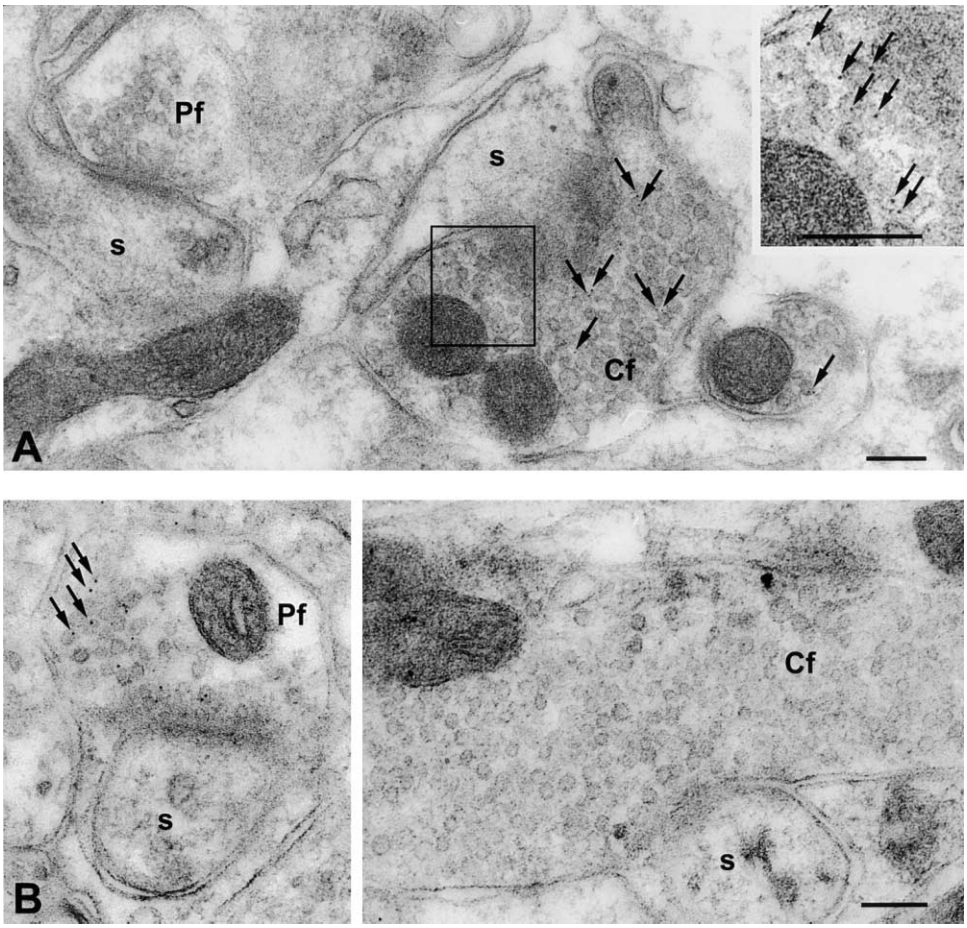

Figure 6. VGLUT1 and 2 Localize to Synaptic Vesicles in Distinct Sets of Excitatory Nerve Terminals

(A) Immunogold localization in the molecular layer of the cerebellar cortex shows DNPI/VGLUT2 on synaptic vesicles in climbing fiber boutons (Cf), but not in parallel fiber boutons (Pf). Several of the gold particles are indicated (arrows). There is no apparent selectivity of labeling among vesicles depending on their localization. Note the lack of particles over other tissue elements, including postsynaptic dendritic spines (s) of Purkinje cells. Inset: high-magnification view of a square in the main panel more clearly shows the small gold particles.

(B) VGLUT1 localizes to synaptic vesicles in parallel fiber boutons (left panel), but not in climbing fiber boutons (right panel).

Scale bars: 200 nm.

also appears in the cerebellar cortex, a rhombencephalic structure, and VGLUT2 in layer IV of the cortex. Thus, the decision to express VGLUT1 or 2 does not coincide with an easily identifiable developmental event.

The complementary expression of VGLUT1 and 2 suggests distinct physiological roles in excitatory neurotransmission. However, we have not detected a clear difference in the characteristics of transport between the two isoforms. Both exhibit a similar apparent affinity for glutamate and a biphasic dependence on chloride. They both also rely predominantly on $\Delta\Psi$ but clearly depend on ΔpH as well, and both fail to recognize aspartate. VGLUT1 and 2 may thus differ in regulation rather than intrinsic transport activity.

The differential expression of VGLUT1 and 2 appears to correlate with one measurable property of synapses, the probability of transmitter release. In the cerebellum, climbing fiber synapses show an extremely high probability of release and express VGLUT2, whereas parallel fiber synapses onto the same population of Purkinje cells exhibit a lower probability of release and express VGLUT1 (Dittman and Regehr, 1998). In the brainstem, sensory neurons required to relay information with high fidelity also express VGLUT2. Thalamocortical projections expressing VGLUT2 also show a higher probability of release than intracortical projections presumably expressing VGLUT1 (Gil et al., 1999). Hippocampal synapses, which generally express VGLUT1, show a variable but generally low probability of release (Hessler et al., 1993; Rosenmund et al., 1993). Interestingly, the probability of transmitter release at CA1 synapses appears to decline during early postnatal development (Bolshakov and Siegelbaum, 1995), and VGLUT1 expression upregulates dramatically during this time (Ni et al., 1995) whereas VGLUT2 remains constant (Aihara et al., 2000). Thus, VGLUT2 appears to be expressed at synapses with a high release probability and VGLUT1 at synapses with lower probabilities of release.

How might the expression of VGLUT1 and 2 contribute to differences in the probability of transmitter release? The results suggest that differences in trafficking may be responsible. Differential centrifugation of brain extracts

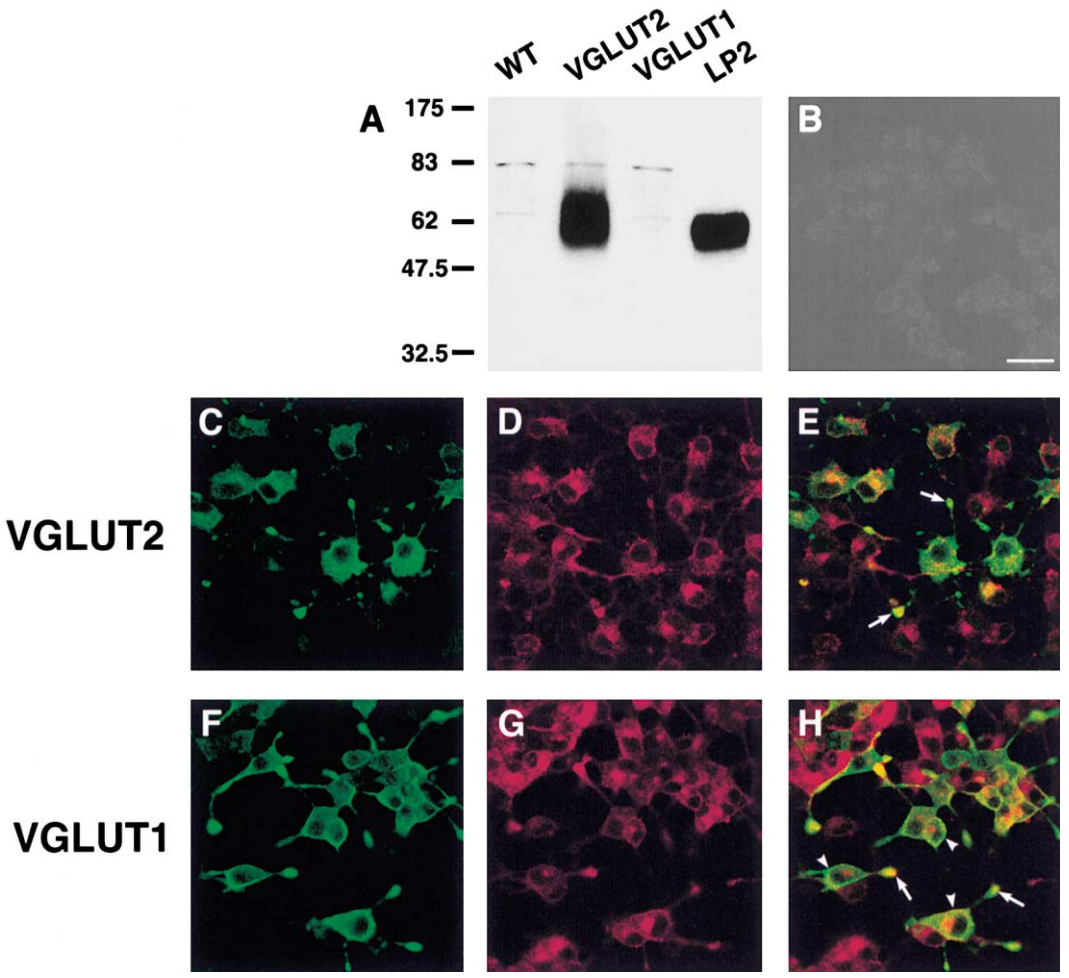

Figure 7. Heterologous Expression of DNPI in PC12 Cells

(A) Western analysis of extracts prepared from untransfected (WT) PC12 cells, cells stably expressing DNPI/VGLUT2, VGLUT1, and the LP2 fraction of rat brain membranes shows that an antibody raised against the C terminus of DNPI recognizes specifically DNPI.

(B–H) Localization of DNPI/VGLUT2 and VGLUT1 in PC12 cells by confocal microscopy. Untransfected cells show no immunoreactivity for DNPI (B). Cells stably expressing DNPI and VGLUT1 were double stained with the appropriate antibody for transporter ([C and F], green) and synaptophysin ([D and G], red). Both DNPI and VGLUT1 colocalize with synaptophysin in processes (arrows) ([E and H], overlay). However, they show different patterns of immunostaining within PC12 cell bodies. DNPI shows a more diffuse cytoplasmic location than VGLUT1, which has a peripheral somatic distribution (arrowheads). Scale bar: 25 μm (E–H).

shows the localization of VGLUT2 to a population of crude membranes lighter than synaptosomes. In addition, VGLUT2 has a more diffuse and VGLUT1 a more peripheral distribution in the cell bodies of PC12 cells. Even though both clearly localize to synaptic vesicles, the VGLUT proteins thus appear to differ in either the rate of internalization from the cell surface or their fate after endocytosis. The C terminus of VGLUT1 indeed contains two polyproline motifs which are absent from VGLUT2, and the interaction of polyproline motifs in other proteins with proteins containing src homology 3 (SH3) domains has been shown to participate in synaptic vesicle recycling (Shupliakov et al., 1997). Differences in VGLUT expression may therefore contribute to the different release properties observed at different synapses.

Experimental Procedures

Molecular Cloning of DNPI/VGLUT2

A fragment of the mouse expressed sequence tag AI841371 was amplified by polymerase chain reaction (PCR) from mouse brain poly-A^+ mRNA and used to screen a rat brain cDNA library, resulting in the isolation of a partial cDNA clone (nucleotides 970–3982 of rat DNPI, accession number AAF76223). To reconstruct the full open reading frame, the missing segment was amplified from rat brain cDNA by PCR and ligated at a common HindIII site (nucleotide 1213). Sequence analysis on both strands confirmed the identity to rat DNPI (AAF76223).

In Situ Hybridization

cDNA fragments corresponding to unique carboxy-terminal tail and 3′ untranslated regions of the rat DNPI cDNA (nucleotides 2017–2358) and the rat BNPI cDNA (nucleotides 1644–2024) (31% nucleotide identity with <5 contiguous identical bases) were amplified by

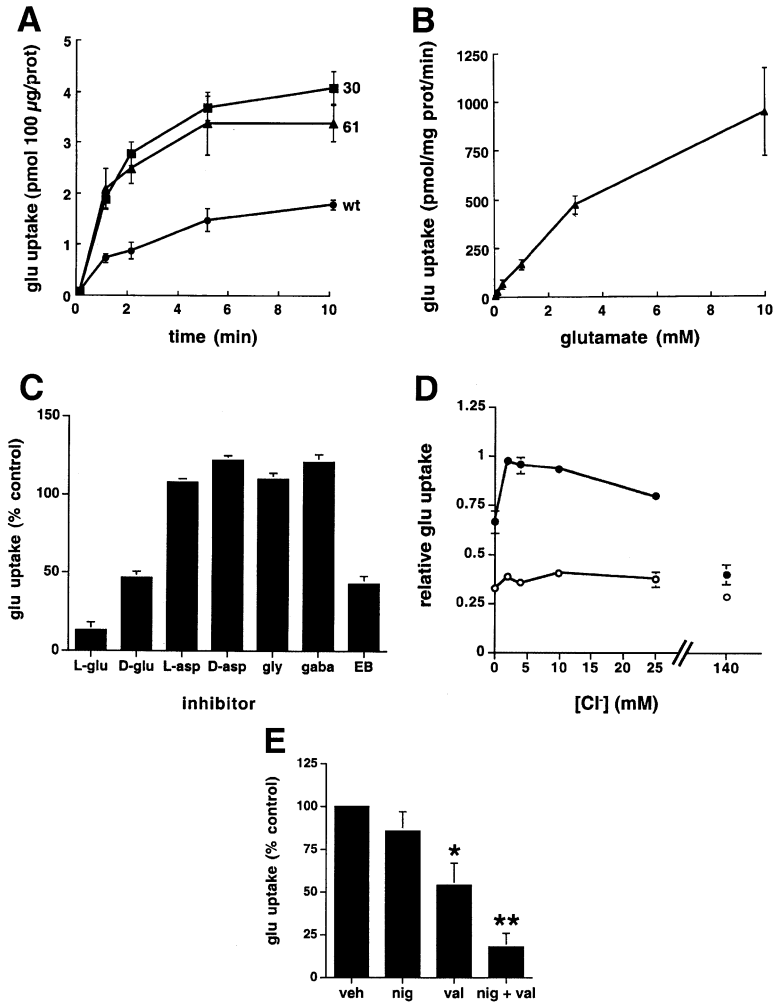

Figure 8. DNPI Catalyzes Vesicular Glutamate Transport

(A) Membranes prepared from two stable PC12 transformants expressing DNPI/VGLUT2 (lines 30 and 61) accumulate substantially more [^{3}H]L-glutamate than membranes from untransfected cells (WT). The results represent the average from three experiments performed in duplicate using membranes from different vesicle preparations. The error bars represent the standard error of the mean.

(B) The initial rate of uptake (V_0) (at 1 min) saturates with increasing concentrations of L-glutamate (0.03–10 mM). Specific uptake was determined at each glutamate concentration by subtracting the background uptake by untransfected cell membranes from total uptake by membranes expressing DNPI. Lineweaver-Burke analysis indicates a Km 4.7 ± 0.7 mM. The results represent the average of three experiments each performed in triplicate, and the error bars the standard error of the mean.

(C) L-glutamate (L-glu), but not L-aspartate (L-asp), D-aspartate (D-asp), glycine (gly), or γ-aminobutyric acid (gaba) (all at 10 mM) markedly inhibits specific DNPI-mediated uptake of [^{3}H]L-glutamate at 5 min. D-glutamate (D-glu) (10 mM) and Evans Blue (EB) (4.5 μM) also significantly inhibit DNPI-mediated [^{3}H]L-glutamate uptake. The results are expressed as a percentage of specific [^{3}H]L-glutamate accumulated in the absence of inhibitor and represent the average ± SEM of at least four independent determinations.

(D) The uptake of [^{3}H]L-glutamate at 5 min by membranes expressing DNPI (closed circles) exhibits a biphasic dependence on chloride concentration. Untransfected cells (open circles) show no chloride dependence. Although specific uptake can be detected in the absence of added chloride, maximal uptake occurs at a chloride concentration of ~2 mM. In contrast, little or no specific uptake is detectable at 140 mM chloride. Activity was normalized to maximal uptake by the transfected cell membranes. Data represent the average ± SEM of three experiments each performed in triplicate, with several of the smaller error bars obscured by the symbol indicating the mean.

(E) Uptake of [^{3}H]L-glutamate by membranes expressing DNPI depends more on membrane potential than on the pH gradient. Membranes were preloaded with 4 mM KCl, and specific uptake at 5 min was determined in the presence of either 1% ethanol (veh), 5 μM nigericin (nig), 20 μM valinomycin (val), or 5 μM nigericin and 20 μM valinomycin (nig + val). The uptake by membranes from untransfected cells was subtracted from uptake by membranes expressing DNPI. The results indicate the percentage of specific uptake obtained in the absence of ionophore (veh) and represent the average ± SEM of three experiments each performed in triplicate. *$p < 0.05$ compared to vehicle; **$p < 0.01$ compared to valinomycin alone (two-tailed, paired Student's t test).

PCR and subcloned into the RNA expression plasmid pBluescriptII (Stratagene). ^{35}S-labeled antisense and sense strand RNA probes were prepared by in vitro transcription of the linearized templates to a specific activity $>10^9$ cpm/μg. In situ hybridization was conducted as previously described (Fremeau et al., 1992) by postfixation in 4% paraformaldehyde (PFA) of rat brain sections from 21-day-old males (Sprague-Dawley) and hybridization to ^{35}S-labeled single-stranded RNA probes in 50% formamide for 16–18 hr at 53°C. The sections were then treated with RNase A (50 μg/ml for 60 min at 37°C), washed at high stringency (0.1× SSC for 3 hr at 50°C), exposed to BioMax MS film (Kodak) for 3 days, dipped in NTB2 nuclear track emulsion (Kodak), and exposed for 4–6 weeks.

Polyclonal Antibody Production

The pGEX bacterial expression system (Pharmacia Biotech) was used to produce a glutathione S-transferase (GST) fusion protein containing the carboxy-terminal 64 amino acids (residues 519–582) of rat DNPI. The 3′ end of the protein-coding region (nucleotides 2017–2220) was amplified from the rat DNPI cDNA by PCR using primers (5′-GGGAATTCATTCATGAAGATGAACTGGATGAA and 5′-GGCTCGAGCTAGCTTCGTTATGAATAATCATC) and subcloned into pGEX-5X-1 at EcoRI and XhoI sites. The fusion protein was produced in the XL1-Blue strain of *E. coli*, purified over glutathione-sepharose, and used to generate polyclonal rabbit antisera (Quality Controlled Biochemicals).

Immunocytochemistry

23-day-old Sprague-Dawley rats (Charles River) were anesthetized with pentobarbital, perfused with 4% PFA/PBS, and the brains were removed, postfixed by immersion in 4% PFA/PBS overnight, equilibrated with 30% sucrose/PBS, and frozen. Coronal sections (40 μm) were immunostained with the rabbit antibody to VGLUT2-GST after preadsorption with 20 μg/ml VGLUT1-GST. Adjacent sections were immunostained in parallel with rabbit anti-VGLUT1-GST antibody after preadsorption with 20 μg/ml VGLUT2-GST. The antibody deposits were visualized with biotinylated goat anti-rabbit secondary antibody, avidin-biotin-peroxidase (Vector), and H_2O_2/diaminobenzidine as previously described (Bellocchio et al., 1998) but with-

out $NiSO_4$. Alternatively, brains of Wistar rats perfusion fixed with 4% PFA in 0.1 M sodium phosphate buffer (pH 7.4) (or, for electron microscopy, with the addition of 0.5% glutaraldehyde) were sectioned sagittally at 40 μm by a Vibratome. The sections were processed for light and electron microscopic immunoperoxidase as described (Chaudhry et al., 1998), except that for light microscopy 0.5% Triton X-100 was included with the antibodies (prepared as above).

Postembedding immunogold localization was performed generally as described (Chaudhry et al., 1995). Specifically, rats were perfused with 4% PFA + 0.1% glutaraldehyde, and brain tissue was embedded by freeze-substitution in Lowicryl HM20. Ultrathin sections (70 nm) mounted on Formvar-coated nickel grids were etched on drops of fresh 1% H_2O_2 in ultrapure water for 0.5 hr at room temperature in the dark, blocked with 5% normal goat serum + 2% BSA in 0.05 M Tris-HCl (pH 7.6), 0.14 M NaCl, 0.01% Triton X-100 (TBSX) for 1 hr at room temperature, and incubated with the primary antibodies in the blocking solution overnight at 4°C. Anti-VGLUT1-GST was diluted 1:100, anti-VGLUT2-GST was diluted 1:500 and preadsorbed with 40 μg/ml of the other VGLUT-GST fusion protein. After rinsing in TBSX, the sections were incubated with goat anti-rabbit Fab-fragments coupled to 5 nm gold particles (British BioCell International, Cardiff, UK), diluted 1:20 in TBSX with 2% BSA for 90 min at room temperature. After rinsing, the sections were contrasted with uranyl acetate and lead citrate and observed in a Philips CM10 electron microscope.

Subcellular Fractionation and Western Analysis

Synaptosomes were prepared from whole rat brain as previously described (Huttner et al., 1983). Briefly, synaptosomes (P2) were purified by differential centrifugation and lysed by hypotonic shock to release synaptic vesicles. Heavy membranes (including the plasma membrane) were then sedimented at 33,000 × g for 20 min (LP1) and the supernatant (LS1) sedimented at 251,000 × g for 210 min to collect lighter membranes including synaptic vesicles (LP2).

Velocity sedimentation through glycerol was performed as previously described (Clift-O'Grady et al., 1990). Briefly, lysed synaptosomes were sedimented through 5%–25% glycerol at 195,600 × g in an SW41 rotor (Beckman) for 1 hr at 4°C.

The fractions obtained by differential centrifugation or velocity sedimentation were assayed for protein content by the Bradford method (Bio-Rad), separated by electrophoresis through SDS-acrylamide, electroblotted to nitrocellulose, and immunostained as previously described (Bellocchio et al., 1998). VGLUT2 and VGLUT1 antibodies were used at a dilution of 1:2000 after adsorption with liver acetone powder (ICN) to reduce background. Synaptophysin was detected with a rabbit polyclonal antibody (Zymed) at 1:10,000, syntaxin with a mouse monoclonal antibody (Sigma) at 1:2000, and the NR1 subunit of the NMDA receptor (Chemicon) at 0.5 μg/ml. The immunoreactive deposits were detected by enhanced chemiluminescence (Pierce).

Heterologous Expression, Membrane Preparation, and Transport Assay

PC12 cells were grown in Dulbecco's modified Eagle's medium containing 10% equine serum, 5% calf serum, and transfected by electroporation with the rat DNPI/VGLUT2 cDNA subcloned in the pcDNA3 vector containing an RSV promoter (Krantz et al., 2000). Stable transformants were selected for resistance to the neomycin analog G418 (500 μg/ml) and screened by immunofluorescence with the DNPI antibody, resulting in the identification of two independent clones with more than 80% of the cells expressing DNPI.

For membrane preparation, untransfected and DNPI-expressing PC12 cells were grown on 15 cm plates, washed with calcium- and magnesium-free PBS, collected in 0.32 M sucrose/10 mM HEPES-KOH, (pH 7.4) (SH buffer) containing protease inhibitors (2 μg/ml leupeptin, 1 μg/ml pepstatin, 1 μg/ml E64, 0.2 mM diisopropylfluorphosphate, 2 μg/ml aprotinin, and 1.25 mM MgEGTA), homogenized using a ball bearing device, and the homogenate sedimented at 1000 × g for 5 min to remove nuclei and debris. The supernatant was then sedimented at 27,000 × g for 35 min to remove heavier membranes. The remaining light membranes including small synaptic-like microvesicles were then sedimented at 210,000 × g for 1 hr. The pellet was resuspended in SH buffer with protease inhibitors at ~10 mg protein/ml.

To initiate the transport reaction, 20 μl membranes (~200 μg protein) were added to 180 μl SH buffer containing 4 mM KCl, 4 mM $MgSO_4$, 4 mM ATP, and 100 μM [^{3}H]L-glutamate, with other additions noted in the text and figure legends. The reaction mixture was incubated at 29°C for varying intervals, uptake was terminated by rapid filtration through Supor-200 membranes (Gelman), and the filters were washed rapidly four times with 1.5 ml cold 0.155 M potassium tartrate/10 mm HEPES-KOH (pH 7.4) before measuring the bound radioactivity by scintillation counting in 3 ml Cytoscint (ICN). Uptake specifically mediated by DNPI/VGLUT2 was determined by subtracting the background uptake of untransfected cell membranes from the uptake by transfected cell membranes. To examine the chloride dependence of transport, varying proportions of 0.14 M K gluconate and 0.14 M KCl were mixed in the standard reaction buffer (without sucrose) to vary the chloride concentration and maintain constant osmolarity. The ionophores nigericin and valinomycin used in Figure 7E were prepared as 200× stock solutions in ethanol. The final ethanol concentration in the reaction mixture was 1%.

Acknowledgments

We thank S. Pleasure, M. Stryker, R. Nicoll, and the members of the Edwards laboratory for helpful discussions; F.A. Chaudhry and V. Gundersen for advice with the immunocytochemistry; and the EU (I.P.), NRC (G.O.N., J.S.-M.), HHMI (E.E.B.), NINDS (R.T.F., M.D.T., R.J.R.), and NIMH (R.H.E.) for their support.

Received March 7, 2001; revised May 31, 2001.

References

Aihara, Y., Mashima, H., Onda, H., Hisano, S., Kasuya, H., Hori, T., Yamada, S., Tomura, H., Yamada, Y., Inoue, I., et al. (2000). Molecular cloning of a novel brain-type Na^+-dependent inorganic phosphate cotransporter. J. Neurochem. *74*, 2622–2625.

Amaral, D.G., and Witter, M.P. (1995). Hippocampal formation. In The Rat Nervous System, Second Edition., G. Paxinos, ed. (San Diego: Academic Press), pp. 443–493.

Araque, A., Li, N., Doyle, R.T., and Haydon, P.G. (2000). SNARE protein-dependent glutamate release from astrocytes. J. Neurosci. *20*, 666–673.

Avery, L. (1993). The genetics of feeding in Caenorhabditis elegans. Genetics *133*, 897–917.

Bajjalieh, S.M., Peterson, K., Linial, M., and Scheller, R.H. (1993). Brain contains two forms of synaptic vesicle protein 2. Proc. Natl. Acad. Sci. USA *90*, 2150–2154.

Bellocchio, E.E., Hu, H., Pohorille, A., Chan, J., Pickel, V.M., and Edwards, R.H. (1998). The localization of the brain-specific inorganic phosphate transporter suggests a specific presynaptic role in glutamatergic transmission. J. Neurosci. *18*, 8648–8659.

Bellocchio, E.E., Reimer, R.J., Fremeau, R.T.J., and Edwards, R.H. (2000). Uptake of glutamate into synaptic vesicles by an inorganic phosphate transporter. Science *289*, 957–960.

Bezzi, P., Carmignoto, G., Pasti, L., Vesce, S., Rossi, D., Rizzini, B.L., Pozzan, T., and Volterra, A. (1998). Prostaglandins stimulate calcium-dependent glutamate release in astrocytes. Nature *391*, 281–285.

Bolshakov, V.Y., and Siegelbaum, S.A. (1995). Regulation of hippocampal transmitter release during development and long-term potentiation. Science *269*, 1730–1734.

Bröer, S., Schuster, A., Wagner, C.A., Bröer, A., Forster, I., Biber, J., Murer, H., Werner, A., Lang, F., and Busch, A.E. (1998). Chloride conductance and Pi transport are separate functions induced by the expression of NaPi-1 in Xenopus oocytes. J. Memb. Biol. *164*, 71–77.

Busch, A.E., Schuster, A., Waldegger, S., Wagner, C.A., Zempel, G., Broer, S., Biber, J., Murer, H., and Lang, F. (1996). Expression of a renal type I sodium/phosphate transporter (NaPi-1) induces a con-

ductance in Xenopus oocytes permeable for organic and inorganic anions. Proc. Natl. Acad. Sci. USA *93*, 5347–5351.

Carlson, M.D., Kish, P.E., and Ueda, T. (1989a). Characterization of the solubilized and reconstituted ATP-dependent vesicular glutamate uptake system. J. Biol. Chem. *264*, 7369–7376.

Chaudhry, F.A., Lehre, K.P., van Lookeren Campagne, M., Otterson, O.P., Danbolt, N.C., and Storm-Mathisen, J. (1995). Glutamate transporters in glial plasma membranes: highly differentiated localizations revealed by quantitative ultrastructural immunocytochemistry. Neuron *15*, 711–720.

Chaudhry, F.A., Reimer, R.J., Bellocchio, E.E., Danbolt, N.C., Osen, K.K., Edwards, R.H., and Storm-Mathisen, J. (1998). The vesicular GABA transporter VGAT localizes to synaptic vesicles in sets of glycinergic as well as GABAergic neurons. J. Neurosci. *18*, 9733–9750.

Clift-O'Grady, L., Linstedt, A.D., Lowe, A.W., Grote, E., and Kelly, R.B. (1990). Biogenesis of synaptic vesicle-like structures in a pheochromocytoma cell line PC12. J. Cell Biol. *110*, 1693–1703.

Cornwall, J., and Phillipson, O.T. (1988a). Afferent projections to the dorsal thalamus of the rat as shown by retrograde lectin transport—I. The mediodorsal nucleus. Neurosci. *24*, 1035–1049.

Cornwall, J., and Phillipson, O.T. (1988b). Afferent projections to the dorsal thalamus of the rat as shown by retrograde lectin transport. II. The midline nuclei. Brain Res. Bull. *21*, 147–161.

Dan, Y., Song, H.J., and Poo, M.M. (1994). Evoked neuronal secretion of false transmitters. Neuron *13*, 909–917.

Dent, J.A., Davis, M.W., and Avery, L. (1997). avr-15 encodes a chloride channel subunit that mediates inhibitory glutamatergic neurotransmission and ivermectin sensitivity in Caenorhabditis elegans. EMBO J. *16*, 5867–5879.

Disbrow, J.K., Gershten, M.J., and Ruth, J.A. (1982). Uptake of L-[^{3}H] glutamic acid by crude and purified synaptic vesicles from rat brain. Biochem. Biophys. Res. Commun. *108*, 1221–1227.

Dittman, J.S., and Regehr, W.G. (1998). Calcium dependence and recovery kinetics of presynaptic depression at the climbing fiber to Purkinje cell synapse. J. Neurosci. *18*, 6147–6162.

Fremeau, R.T.J., Caron, M.G., and Blakely, R.D. (1992). Molecular cloning and expression of a high affinity L-proline transporter expressed in putative glutamatergic pathways of rat brain. Neuron *8*, 915–926.

Fykse, E.M., Takei, K., Walch-Solimena, C., Geppert, M., Jahn, R., De Camilli, P., and Südhof, T.C. (1993). Relative properties and localizations of synaptic vesicle protein isoforms: the case of the synaptophysins. J. Neurosci. *13*, 4997–5007.

Gil, Z., Connors, B.W., and Amitai, Y. (1999). Efficacy of thalamocortical and intracortical synaptic connections: quanta, innervation, and reliability. Neuron *23*, 385–397.

Glinn, M., Ni, B., Irwin, R.P., Kelley, S.W., Lin, S.Z., and Paul, S.M. (1998). Inorganic Pi increases neuronal survival in the acute early phase following excitotoxic/oxidative insults. J. Neurochem. *70*, 1850–1858.

Hessler, N.A., Shirke, A.M., and Malinow, R. (1993). The probability of transmitter release at a mammalian central synapse. Nature *366*, 569–572.

Hisano, S., Hoshi, K., Ikeda, Y., Maruyama, D., Kanemoto, M., Ichijo, H., Kojima, I., Takeda, J., and Nogami, H. (2000). Regional expression of a gene encoding a neuron-specific Na^+-dependent inorganic phosphate transporter (DNPI) in the rat forebrain. Mol. Brain Res. *83*, 34–43.

Huttner, W.B., Schiebler, W., Greengard, P., and DeCamilli, P. (1983). Synapsin I (Protein I), a nerve terminal-specific phosphoprotein. III. Its association with synaptic vesicles studied in a highly purified synaptic vesicle preparation. J. Cell Biol. *96*, 1374–1388.

Krantz, D.E., Waites, C., Oorschot, V., Liu, Y., Wilson, R.I., Tan, P.K., Klumperman, J., and Edwards, R.H. (2000). A phosphorylation site in the vesicular acetylcholine transporter regulates sorting to secretory vesicles. J. Cell Biol. *149*, 379–396.

Lee, R.Y., Sawin, E.R., Chalfie, M., Horvitz, H.R., and Avery, L. (1999). EAT-4, a homolog of a mammalian sodium-dependent inorganic phosphate cotransporter, is necessary for glutamatergic neurotransmission in caenorhabditis elegans. J. Neurosci. *19*, 159–167.

Liu, Y., and Edwards, R.H. (1997a). The role of vesicular transport proteins in synaptic transmission and neural degeneration. Annu. Rev. Neurosci. *20*, 125–156.

Mancini, G.M., de Jonge, H.R., Galjaard, H., and Verheijen, F.W. (1989). Characterization of a proton-driven carrier for sialic acid in the lysosomal membrane. Evidence for a group-specific transport system for acidic monosaccharides. J. Biol. Chem. *264*, 15247–15254.

Maycox, P.R., Deckwerth, T., Hell, J.W., and Jahn, R. (1988). Glutamate uptake by brain synaptic vesicles. Energy dependence of transport and functional reconstitution in proteoliposomes. J. Biol. Chem. *263*, 15423–15428.

Naito, S., and Ueda, T. (1983). Adenosine triphosphate-dependent uptake of glutamate into protein I-associated synaptic vesicles. J. Biol. Chem. *258*, 696–699.

Newman, E.A., and Zahs, K.R. (1998). Modulation of neuronal activity by glial cells in the retina. J. Neurosci. *18*, 4022–4028.

Ni, B., Rosteck, P.R., Nadi, N.S., and Paul, S.M. (1994). Cloning and expression of a cDNA encoding a brain-specific Na^+-dependent inorganic phosphate cotransporter. Proc. Natl. Acad. Sci. USA *91*, 5607–5611.

Ni, B., Wu, X., Yan, G.-M., Wang, J., and Paul, S.M. (1995). Regional expression and cellular localization of the Na^+-dependent inorganic phosphate cotransporter of rat brain. J. Neurosci. *15*, 5789–5799.

Otis, T.S. (2001). Vesicular glutamate transporters in cognito. Neuron *29*, 11–14.

Raizen, D.M., and Avery, L. (1994). Electrical activity and behavior in the pharynx of *Caenorhabditis elegans*. Neuron *12*, 483–495.

Reimer, R.J., Fon, E.A., and Edwards, R.H. (1998). Vesicular neurotransmitter transport and the presynaptic regulation of quantal size. Curr. Opin. Neurobiol. *8*, 405–412.

Rosenmund, C., Clements, J.D., and Westbrook, G.L. (1993). Nonuniform probability of glutamate release at a hippocampal synapse. Science *262*, 754–757.

Schuldiner, S., Shirvan, A., and Linial, M. (1995). Vesicular neurotransmitter transporters: from bacteria to humans. Physiol. Rev. *75*, 369–392.

Shupliakov, O., Low, P., Grabs, D., Gad, H., Chen, H., David, C., Takei, K., De Camilli, P., and Brodin, L. (1997). Synaptic vesicle endocytosis impaired by disruption of dynamin-SH3 domain interactions. Science *276*, 259–263.

Stanfield, B.B., and Cowan, W.M. (1984). An EM autoradiographic study of the hypothalamo-hippocampal projection. Brain Res. *309*, 299–307.

Storm-Mathisen, J., Leknes, A.K., Bore, A.T., Vaaland, J.L., Edminson, P., Haug, F.M., and Ottersen, O.P. (1983). First visualization of glutamate and GABA in neurones by immunocytochemistry. Nature *301*, 517–520.

Sulzer, D., Joyce, M.P., Lin, L., Geldwert, D., Haber, S.N., Hattori, T., and Rayport, S. (1998). Dopamine neurons make glutamatergic synapses in vitro. J. Neurosci. *18*, 4588–4602.

Takamori, S., Rhee, J.S., Rosenmund, C., and Jahn, R. (2000). Identification of a vesicular glutamate transporter that defines a glutamatergic phenotype in neurons. Nature *407*, 189–194.

van Groen, T., and Wyss, J.M. (1990). The connections of presubiculum and parasubiculum in the rat. Brain Res. *518*, 227–243.

Varoqui, H., Diebler, M.-F., Meunier, F.-M., Rand, J.B., Usdin, T.B., Bonner, T.I., Eiden, L.E., and Erickson, J.D. (1994). Cloning and expression of the vesamicol binding protein from the marine ray *Torpedo*. Homology with the putative vesicular acetylcholine transporter UNC-17 from *Caenorhabditis elegans*. FEBS Lett. *342*, 97–102.

Verheijen, F.W., Verbeek, E., Aula, N., Beerens, C.E., Havelaar, A.C., Joosse, M., Peltonen, L., Aula, P., Galjaard, H., van der Spek, P.J., and Mancini, G.M. (1999). A new gene, encoding an anion transporter, is mutated in sialic acid storage diseases. Nat. Genet. *23*, 462–465.

Wolosker, H., de Souza, D.O., and de Meis, L. (1996). Regulation of glutamate transport into synaptic vesicles by chloride and proton gradient. J. Biol. Chem. *271*, 11726–11731.

Wouterlood, F.G., Saldana, E., and Witter, M.P. (1990). Projection from the nucleus reuniens thalami to the hippocampal region: light and electron microscopic tracing study in the rat with the anterograde tracer Phaseolus vulgaris-leucoagglutinin. J. Comp. Neurol. *296*, 179–203.

Wyss, J.M., Swanson, L.W., and Cowan, W.M. (1979). Evidence for an input to the molecular layer and the stratum granulosum of the dentate gyrus from the supramammillary region of the hypothalamus. Anat. Embryol. *156*, 165–176.